

Avoiding cytotoxicity of transposases by dose-controlled mRNA delivery

Melanie Galla¹, Axel Schambach¹, Christine S. Falk², Tobias Maetzig¹, Johannes Kuehle¹, Kathrin Lange³, Daniela Zychlinski¹, Niels Heinz¹, Martijn H. Brugman⁴, Gudrun Göhring³, Zsuzsanna Izsvák^{5,6}, Zoltán Ivics^{5,6} and Christopher Baum^{1,*}

¹Department of Experimental Hematology, ²Institute of Transplantation Immunology, ³Institute of Cell and Molecular Pathology, Hannover Medical School, Hannover, Germany, ⁴Department of Immunohematology and Blood Transfusion, Leiden University Medical Center, Leiden, The Netherlands, ⁵Division of Mobile DNA, Max Delbrück Center for Molecular Medicine, Berlin, Germany and ⁶Department of Human Genetics, University of Debrecen, Debrecen, Hungary

Received December 7, 2010; Revised and Accepted April 28, 2011

ABSTRACT

The *Sleeping Beauty* (SB) transposase and its newly developed hyperactive variant, SB100X, are of increasing interest for genome modification in experimental models and gene therapy. The potential cytotoxicity of transposases requires careful assessment, considering that residual integration events of transposase expression vectors delivered by physicochemical transfection or episomal retroviral vectors may lead to permanent transposase expression and resulting uncontrollable transposition. Comparing retrovirus-based approaches for delivery of mRNA, episomal DNA or integrating DNA, we found that conventional SB transposase, SB100X and a newly developed codon-optimized SB100Xo may trigger premitotic arrest and apoptosis. Cell stress induced by continued SB overexpression was self-limiting due to the induction of cell death, which occurred even in the absence of a co-transfected transposable element. The cytotoxic effects of SB transposase were strictly dose dependent and heralded by induction of p53 and c-Jun. Inactivating mutations in SB's catalytic domain could not abrogate cytotoxicity, suggesting a mechanism independent of DNA cleavage activity. An improved approach of retrovirus particle-mediated mRNA transfer allowed transient and dose-controlled expression of SB100X, supported efficient transposition and prevented cytotoxicity. Transposase-mediated gene transfer can thus be

tuned to maintain high efficiency in the absence of overt cell damage.

INTRODUCTION

The *Sleeping Beauty* (SB) system (1), consisting of a transposon vector with a gene of interest and a *trans*-acting transposase, has been developed as a promising alternative to integrating retrovirus (iRV)-based gene delivery vehicles (2,3). The recently introduced hyperactive SB100X transposase greatly improved the prospects for efficient gene transfer into many cell types that are of interest for both, basic research and gene therapy (2). Compared to the first generation conventional SB (cSB), which was resurrected from a deficient fish transposon (1), SB100X contains several mutations that collaboratively increase its transposition activity without major changes of the transposon's close-to-random integration pattern. Provided that suitable transfection methods are available for a given target cell type, SB100X reaches stable gene transfer rates that were previously only achieved by retrovirus-based vectors (2), including the more recent generations of lentiviral vectors (4).

The SB transposase is typically transiently supplied to prevent remobilization of integrated transposable elements within the genome of target cells. Previous studies have indicated that the expression level of the transposase requires careful adjustment to avoid overproduction inhibition, which may be triggered by the accumulation of transposase oligomers incapable of DNA binding possibly due to incorrect folding of the protein (5,6). Improvements of the delivery systems have thus gained increasing interest. Various physicochemical transfection methods,

*To whom correspondence should be addressed. Tel: +49 511 532 6067; Fax: +49 511 532 6068; Email: baum.christopher@mh-hannover.de

DNA-based viral vectors or episomal lentiviral vectors (eLV) deliver DNA transiently. However, physicochemical transfection may induce substantial toxicity in primary cell types that may limit a wider applicability of SB. Another concern is that DNA transfection, adenoviral vectors and eLV have a residual potency of stable gene transfer which can affect 0.01–3% of the targeted cell population (7–9). In the context of a transposon system, this could lead to permanent genomic insertion of a transposase source, with uncontrollable transposition and congruent genomic instability. Transfecting *in vitro* generated transposase mRNA has been proposed as an alternative, transient delivery method (10), but it remained unclear how this approach can be adjusted to reach homogenous expression levels in the transfected cell population.

In previous work, we have introduced a retrovirus particle-mediated approach of mRNA transduction [named RMT, (11)]. This method exploits the fact that retroviral particles package two copies of their plus-stranded, capped and polyadenylated mRNA genome, which may serve as a translation template in transduced cells unless it undergoes reverse transcription (RT). RMT vectors, containing a mutated artificial primer binding site (aPBS) that does not match any naturally occurring tRNA, efficiently block RT (12), and instead promote protein synthesis. A prerequisite for RMT is that the retroviral mRNA is introduced in a configuration that supports efficient translation, as shown for gammaretroviral vectors (7,11,13). Lentiviral vectors are less well suited for RMT because their 5' untranslated region is relatively large with many aberrant reading frames preceding the site used to introduce the sequences of interest (4). Demonstrating that the retroviral mRNA genome is the active principle of RMT, it was shown to be sensitive to expression of short-hairpin RNAs in the target cells (7). In comparison with eLV (14), RMT leads to a more rapid onset, lower level and shorter duration of expression, and fully avoids residual integration events (7).

In the present study, we examined the consequences of three retrovirus-based transposase delivery systems—transient expression at a relatively low level (RMT), a more prolonged and more potent, mostly transient DNA-based expression from integrase-defective episomal gammaretroviral and lentiviral vectors (eRV and eLV) and permanent expression from integrating gammaretroviral vectors (iRV)—in terms of transposition efficacy and potential cytotoxic side-effects. To enhance the potency of RMT, we modified the expression vectors and codon-optimized the SB100X coding sequence. To examine the specificity of potential cytotoxic effects and to assess the versatility of the expression systems, we took the same approaches to express a codon-optimized version of the site-specific FLP recombinase [FLPo, (15)]. We demonstrate a previously unknown cytotoxic effect of high and prolonged SB expression, associated with induction and phosphorylation of p53 and c-Jun. Importantly, cytotoxicity could be avoided by short-term expression of SB, using RMT or dose-controlled transient transfection.

MATERIALS AND METHODS

Vector design

The construction of all retroviral and non-viral expression plasmids that were used in this study is explicitly explained in 'Material and Methods' of the Supplementary Data.

Cell culture and production of retroviral vector supernatants

HeLa, HeLa Fucci [kindly provided by Dr A. Miyawaki (16)], 293 T, SC-1-based FLP reporter cells (17) and the analogously generated HT1080 FLP reporter cells were grown in Dulbecco's modified Eagle's medium (Biochrom, Berlin, Germany) supplemented with 10% fetal calf serum, 1 mM sodium pyruvate (PAA, Coelbe, Germany) and 1% Penicillin/Streptomycin (PAA). Murine induced pluripotent stem (IPS) cells expressing the FLP indicator cassette were cultured on γ -irradiated C3H murine embryonic fibroblasts (MEFs) in mouse embryonic stem (mES) cell medium as recently described (17). For retroviral vector production, 6×10^6 293 T cells were seeded into a 10 cm dish and transfected the next day using the calcium phosphate precipitation method assisted by 25 μ M chloroquine (Sigma Aldrich, Munich, Germany). For gammaretroviral production, 5 μ g iRV, RMT or RBid vector plasmids were cotransfected with expression plasmids for MLV-gag-pol (7 μ g) or integration-defective MLV-gag-pol [D184A, (18)] and the glycoprotein from vesicular stomatitis virus (VSVg/pMD.G; 2 μ g). The production of non-fluorescently labeled RMT and iRV vector supernatants was controlled by additional transfection of 0.5 μ g non-viral pCMV-DsRed-Express expression plasmid (BD Biosciences Clontech, Heidelberg, Germany). Lentiviral vector production was carried out using 5 μ g lentiviral vector expression plasmids together with 12 μ g lentiviral wild-type gag-pol (pcDNA3.gp.4xCTE) or lentiviral integrase-defective gag-pol (pcDNA3.gpD64V.4xCTE, kindly provided by M. Milsom, DKFZ / HI-STEM, Heidelberg, Germany) and 5 μ g pRSV.Rev (kindly provided by T. Hope, Northwestern University, Chicago, IL, USA) and 2 μ g pMD.G. To increase bidirectional vector titers, 5 μ g Nodamura virus B2 protein expression plasmid [NovB2, (18)] was added to the transfection. Supernatants were harvested 36 and 60 h post-transfection and if necessary pooled and concentrated via ultracentrifugation over night at 13 000g and 4°C.

Retroviral cell transduction

Either 2.5×10^4 SC-1-based or 5×10^4 HT1080-based FLP indicator cells were seeded per well of a 24-well-plate. The next day, serial dilutions/MOIs of lentiviral or gammaretroviral supernatants were applied to the cells for 8 h. Transduction was assisted by 4 μ g/ml protamine sulfate (Sigma Aldrich) and centrifugation for 60 min at 400g and 37°C. Murine IPS FLP indicator cells were transduced in single cell suspension. In brief, 3×10^4 murine IPS cells were harvested feeder-free, resuspended in 300 μ l mES cell medium, transferred into a well of a

24-well-suspension plate and transduced in the presence of protamine sulfate with iRV.FLPo and RMT.FLPo particles at an MOI of ~40. The cells were centrifuged as described above, incubated another hour at 37°C and then replated on γ -irradiated C3H MEFs.

RMT-based SB transposition assay

One day prior to transduction, 2×10^5 HeLa cells were seeded per well of a 12-well-plate and transduced at the following day with serial dilutions of concentrated RMT supernatant variants. Twenty-two hours post-transduction, cells were transfected with 600 ng of plasmid DNA that harbors the transposable element expression cassette encoding for EGFP (pSK.IR.SF.EGFP.pA.IR) using polyethyleneimine (PEI; Polysciences, Eppelheim, Germany). The percentage of EGFP⁺ cells were determined 2 and 21 days post-transfection via flow cytometry (fluorescence activated cell sorting [FACS]) and the values were used for calculation of the transposition rates (EGFP⁺ cells at Day 21 divided by EGFP⁺ cells at Day 2). Corresponding iRV-based SB transposase vectors served as positive controls for transposition. Cells that were only transfected with the transposable element plasmid served as control for background integration events.

Northern blot analysis

Using the calcium phosphate transfection method, 293 T cells were cotransfected with 0.5 μ g of pCMV-DsRed-Express (BD Biosciences Clontech), 7 μ g of pMoloney-MLV-*gag-pol* and 5 μ g of conventional or optimized RMT vector plasmids (pSF91aPBS, pRSF91aPBS or pRSF91aPBS+PRE) encoding each either cSB, SB100X or SB100Xo. Thirty-six hours post-transfection, cells were harvested and their total RNA was prepared using the RNazol extraction method (WAK Chemicals, Steinbach, Germany). Using the standard northern blot protocol procedures, 10 μ g of each RNA sample was separated at 2 V/cm in 1% agarose under denaturing conditions, transferred to a Biodyne B membrane (Pall Corporation, Dreieich, Germany) and analyzed via radioactive probing. Specific probes were directed against the 3' SFFV U3 region and 18S RNA (loading control). Radioactive probed membranes were quantified by phosphorimager analysis using the Image Quant TL software (GE Healthcare, Freiburg, Germany).

Western blot analysis

One-million HeLa cells were transduced for 3 h with 40 μ l concentrated integrating (RSF91.cSB.PRE, RSF91.SB100X.PRE or RSF91.SB100Xo.PRE) or RMT (RSF91aPBS.cSB.PRE, RSF91aPBS.SB100X.PRE or RSF91aPBS.SB100Xo.PRE) vector particles. Three hours, 22 h and 12 days post-transduction cells were harvested, washed twice with phosphate-buffered saline and cell lysates were obtained by using radioimmunoprecipitation assay buffer supplemented with proteinase inhibitors (Complete Mini; Roche, Mannheim, Germany). Samples (25 μ g) were separated by sodium dodecyl sulfate–polyacrylamide gel electrophoresis (12.5%), transferred to nitrocellulose membranes (Bio-Rad, Munich,

Germany), and probed with rabbit polyclonal anti-SB transposase (19), goat anti-RLV p30 serum (kindly provided by S.K. Ruscetti, National Cancer Institute at Frederick, Frederick, MD) and mouse anti- α -Tubulin (Sigma Aldrich) in Tris-buffered saline with 0.05% Tween (Carl Roth GmbH, Karlsruhe, Germany) and 3% milk powder (Carl Roth GmbH). Fluorophore-conjugated IRDye 700TMDX anti-mouse IgG (ROCKLAND Immunochemicals, Gilbertsville, PA), IRDye[®] 800CW anti-rabbit IgG (ROCKLAND Immunochemicals) and IRDye[®] 680 donkey anti-goat IgG (LI-COR Biosciences, Bad Homburg, Germany) served as secondary antibodies. Detection and quantification was carried out by using the Odyssey infrared imaging system (LI-COR Biosciences).

Real-time PCR quantification

As for western blotting 1-million HeLa cells were transduced for 3 h with RSF91aPBS.cSB.PRE, RSF91aPBS.SB100X.PRE, RSF91aPBS.SB100Xo.PRE or the corresponding integrating vectors. For real-time RT-PCR, the total RNA of the transduced cells was prepared 3 and 22 h post-transduction using the RNazol extraction method (WAK, Chemicals), liberated from plasmid and genomic DNA and reverse transcribed as previously described (7). For the determination of proviral vector copies, cells were kept in culture and their genomic DNA was extracted at Day 15 post-transduction with the QIAamp DNA blood Mini Kit (Qiagen, Hilden, Germany). Quantitative PCRs were performed on an Applied Biosystems StepOnePlus Real-Time PCR System (Foster City, CA, USA) using the Quantitect Sybr green reagent (Qiagen). The vector's PRE element was detected with oligonucleotide primers 5'-GAGGAGTTGTGGCCCGTTGT-3' and 5'-TGACAGGTGGTGGCAATGCC-3' and normalized either to the signal obtained by the amplification of human beta-actin cDNA with primers 5'-CCTCCCTGGAGAAGAGCTA-3' and 5'-TCCATGCCAGGAAGGAAG-3' (RNA origin) or to the signal obtained by the amplification of a conserved intron of the polypyrimidine tract-binding protein 2 (PTB2) using primers 5'-TCTCCATTCCCTATGTTTCATGC-3' and 5'-GTTCCCGCAGAATGGTGAAGTG-3'. All results were quantified using the comparative threshold cycle method.

Apoptosis assays

The day before transduction, 2×10^5 HeLa or HeLa Fucci cells were seeded and transduced with either 5 μ l concentrated supernatant of unidirectional integrating or RMT vector particles or with integrating or integrase-defective bidirectional vector particles at the depicted MOIs. Cells were harvested either two (unidirectional vectors) or four (bidirectional vectors) days post-transduction, costained with propidium iodide and APC-AnnexinV (BD Biosciences Clontech) according to the manufacturer's protocols and analyzed for apoptotic cells via flow cytometry. Apoptosis was inhibited by culturing the cells until analysis in the presence of 5 μ M Q-VD-OPH, a broad spectrum caspase inhibitor (MP Biomedicals, Heidelberg, Germany).

γ H2AX immunofluorescence

The day before transduction, cover slips (12 mm in diameter, Carl Roth, Karlsruhe, Germany) were placed in wells of a 12-well plate and 2×10^5 HeLa cells per well were seeded on top. The next day, cells were transduced with 5 μ l concentrated supernatant of RSF91.SB100Xo.PRE or RSF91.FLPo.PRE and stained the following day for the appearance of double strand breaks. In brief, cover slips with cells were washed twice with phosphate-buffered saline, fixed with 4% formaldehyde/phosphate-buffered saline, permeabilized with 0.5% Triton X-100/phosphate-buffered saline and stained with anti-phospho-histone H2AX/Ser139 (clone JB301; Millipore, Schwalbach, Germany). AlexaFluor488-conjugated goat anti-mouse IgG (Invitrogen, Darmstadt, Germany) served as secondary antibody. Cell nuclei were costained with blue-fluorescent 4', 6'-Diamidin-2'-phenylindol (DAPI) according to the manufacturer's protocol (SelectFX nuclear labelling kit for fixed cells, Invitrogen). One hundred nuclei per sample were analyzed via fluorescent microscopy for the occurrence of double strand break foci.

Phosphoplex analysis

Multiplex technology was used for determination of the phosphorylation status of selected signaling proteins (ERK1/2, p53, c-Jun and Akt) in cells that were transduced with integrating iRV.SB100X or iRV.EGFP (both RSF91+PRE) vectors. Four hundred thousand HeLa cells were transduced with 5 μ l of concentrated iRV.SB100Xo or iRV.EGFP vector particles. At time points 24, 31, 46 and 54 h post-transduction cells were washed twice with 1 ml ice cold phosphate buffered saline (PAA) and lysed within the culture plates. Cell lysis was carried out using the Bio-Plex Cell Lysis Kit (Bio-Rad, Hercules, USA) according to the manufacturer's instructions. In brief, 125 μ l of cold lysis buffer was added per well, cells were detached with cell scrapers and the resulting lysates transferred into a 1.5 ml reaction tube. Subsequently, samples were gently rotated at 4°C for at least 20 min. To further assist cell lysis, the samples were shock-frosted at -80°C , then thawed on ice and centrifuged at 17000g for 20–25 min at 4°C. The supernatants were stored at -20°C until usage. Before subjecting the samples to Phosphoplex analysis, total protein concentrations of all cell lysates were determined with the Pierce BCA Protein Assay Kit (Thermo Scientific, Bonn, Germany) and adjusted to a concentration of 100 $\mu\text{g}/\text{ml}$ and 50 μ l of each lysate were applied to the bead-based multiplex analysis. Phosphoplex analysis was carried out according to the manufacturer's protocol using the Bio-Plex machine (Bio-Rad) with the Bio-Plex 6.0 software. Mean fluorescence intensity data of at least 50 beads for each total and phosphorylated subset of proteins were collected and applied to statistical analysis (\pm standard deviation of the mean).

Statistical analysis

Data from the experiments are expressed as the means \pm standard deviations. The non-parametric Wilcoxon test

was used for comparison of differences between the indicated groups. A $P < 0.05$ was considered significant.

RESULTS

Vector and protocol modifications to enhance the potency of RMT

Initial experiments performed to deliver the cSB transposase with first-generation RMT vectors (11) had limited success. To elevate RMT titers and therefore the expression of RNA vector genomes (gRNA) in retroviral packaging cells, we first introduced Rous Sarcoma Virus (RSV) enhancer/promoter sequences into the 5' long terminal repeat (LTR) of RMT vector expression plasmids (20). We also added the full-length 900 bp fragment of the Woodchuck Hepatitis Virus post-transcriptional regulatory element (PRE) 3' of the SB cDNA, to enhance mRNA processing and stability (Figure 1A) (21–23). Furthermore, we codon-optimized the hyperactive SB100X reading frame for enhanced initiation of translation [insertion of an optimized Kozak consensus sequence (24)] and efficient codon-usage in human cells, simultaneously deleting cryptic splice and polyadenylation motifs. The resulting optimized cDNA was named SB100Xo (sequence alignment of SB100X and SB100Xo in Supplementary Figure S1). As transposable elements, we developed constructs expressing fluorescent proteins under control of the ubiquitously active Spleen Focus-forming Virus promoter (SFFV) (Figure 1B). RMT vector particles pseudotyped with the Vesicular Stomatitis Virus glycoprotein (VSVg) were produced concentrated and used to transduce HeLa cells. Twenty-two hours later, a transposable element encoding EGFP (pSK.IR.SF.EGFP.pA.IR) was cotransfected using polyethyleneimine (PEI) and the transfection efficiencies were quantified by flow cytometry 2 and 21 days post-transfection. The efficiency of transposition was calculated by determining the ratio of cells expressing the transposable elements at 21 days versus 2 days after delivery. Thus, a value of one reflects a transposition rate of 100%.

Individually and even more collectively, the modifications of the RMT vectors (Figure 1A) greatly enhanced SB transposase expression levels in producer cells (spliced and unspliced vector mRNA, Figure 1C; protein, Supplementary Figure S2A; correlation of mRNA and protein levels, Figure 1D). The improvements of the vector backbone and the codon-optimization cooperated to increase the potency of the RMT approach (Figure 1E and F; Supplementary Figure S2B–D), leading to highly efficient transposition mediated by as little as 5 μ l of $\sim 50 \times$ concentrated RMT vector preparations (Figure 1F). To illustrate the potency, a single vector production from a 10-cm dish of producer cells provided RMT vectors in quantities sufficient for 65 experiments (for 2×10^5 target cells per experiment). Our approach also reproduced the substantially increased potency of SB100X compared to cSB [Supplementary Figure S2B–D, (2)]. Indeed, the increased potency of SB100X was necessary to transfer efficient transposase activity by RMT. When the transposable element encoding EGFP (Figure 1B) was transfected

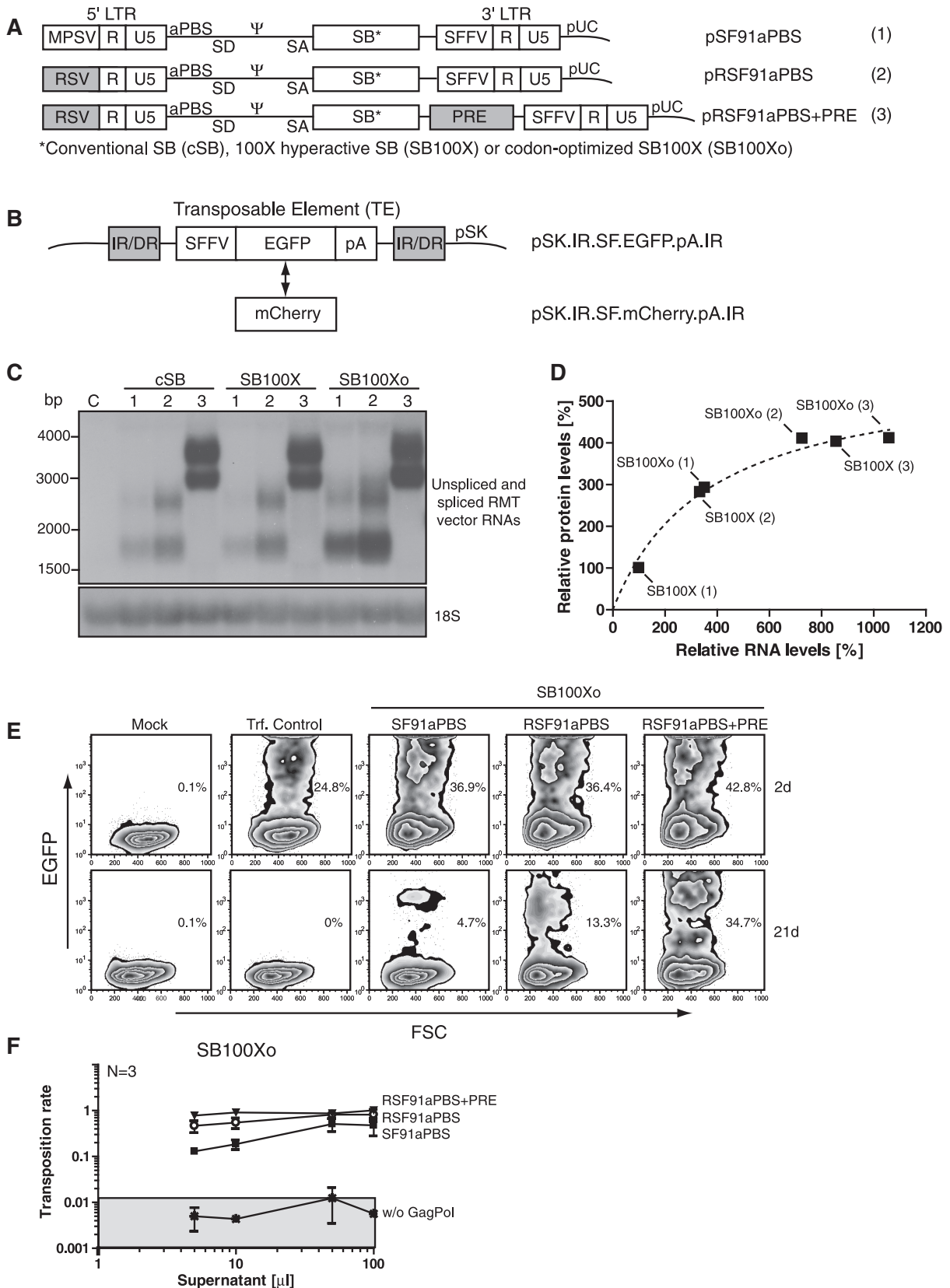


Figure 1. SB transposase expression from new generation RMT vectors allows highly efficient transposition in HeLa cells. (A) Schema of RMT vector plasmids. The original RMT vector is shown in its pUC-plasmid formation (pSF91aPBS, vector 1) and comprises the long terminal repeats (LTR; U3, R, U5), the mutated artificial primer binding site (aPBS), splice donor (SD), retroviral packaging signal (ψ), splice acceptor (SA) and either the conventional, the 100X hyperactive or a codon-optimized version of the 100X Sleeping Beauty (SB) transposase (cSB, SB100X and SB100Xo, respectively). The 5' U3-enhancer-promoter is derived from the Myeloproliferative Sarcoma Virus (MPSV) and the 3' U3 region from the

(continued)

into HeLa cells 22 h after RMT of SB100X or SB100Xo, transposition rates reached up to 100% (Figure 1F and Supplementary Figure S2D).

Since the potency of RMT supernatants is dependent on the viral genomic RNA (gRNA) rather than the viral capsid (p30) content (7), we determined for a subset of RMT vector stocks (RSF91aPBS.cSB.PRE, RSF91aPBS.SB100X.PRE and RSF91aPBS.SB100Xo.PRE), the viral gRNA load in comparison to corresponding RSF91aEGFP.PRE vector preparations. Vector stocks were produced and concentrated under identical conditions, extensively DNase treated and subjected to real-time RT-PCR analysis (Supplementary Figure S2E). On HeLa cells, RSF91aEGFP.PRE preparations had a functional titer of $\sim 1 \times 10^9$ transducing units/ml (data not shown). As already indicated by the RSF91aPBS+PRE vector signal in northern blot analysis of transfected producer cells (Figure 1C), we found that modifications of the SB reading frame (cSB, SB100X and SB100Xo) had no impact on the titer of RMT particle preparations. For practical reasons, we performed further studies with RMT vector doses determined by volume.

To accurately determine the impact of codon-optimization, we coexpressed SB100X or its codon-optimized variant, SB100Xo, in combination with EGFP from bidirectional gammaretroviral (RBid) and lentiviral (LBid) vectors (Supplementary Figure S3A) allowing the identification of SB expressing cells by EGFP fluorescence (18). The vector particles were generated using a gag/pol expression construct harboring a point mutation in the catalytic core domain of the viral integrase, thereby promoting the establishment of extrachromosomal episomal proviral DNA (14). HeLa cells transduced with integration-defective vectors (episomal vectors eLBid and eRBid) of known titer, produced comparable transduction rates. Twenty-two hours post-transduction a transposable element plasmid expressing mCherry (pSK.IR.SF.mCherry.pA.IR, Figure 1B) was transfected and the cells were analyzed via flow cytometry 2 and 14 days post-transfection. Calculation of the transposition rates (ratio of mCherry⁺ cells at Day 14 and EGFP⁺/mCherry⁺ cells at Day 2) revealed an up to 3-fold better performance of SB100Xo in comparison with SB100X

(Supplementary Figure S3B and C). The significantly increased potency of SB100Xo was also documented by RMT with vectors SF91aPBS and RSF91aPBS (Supplementary Figure S2B and C), but undetectable under the saturating expression conditions achieved with the most potent RMT vector, RSF91aPBS+PRE (Supplementary Figure S2D). These experiments revealed that transcriptional and post-transcriptional modifications of the SB expression vector increased the potency to an extent that allowed highly efficient transposition by mRNA delivery.

Using the best-performing vector setting (RSF91aPBS+PRE), we tested whether cotransduction of HeLa cells with RMT of SB100Xo and integration-defective episomal lentiviral vectors delivering the transposable element (eLVTE, Figure 2A) mediates efficient transposition. Such an experimental setup is of interest for cells that are refractory or oversensitive to physico-chemical transfection. Interestingly, combining RMT of SB100Xo and eLVTE resulted in higher transposition rates when compared to settings where SB100Xo was provided by episomal gammaretroviral or lentiviral bidirectional vectors ($\sim 14\%$ versus 7 and 4%, respectively, Figure 2B). Our results compare favorably with two recent publications which explored combinatorial eLV for transposition (25,26). In primary MEFs derived from CF1 mice, we achieved similar rates using RMT, although epigenetic silencing of the transposable element complicated the analysis in these cells (Supplementary Figure S4). The more rapid onset and possibly also the shorter duration and lower level of transposase expression may have accounted for the improved potency of RMT compared to eLV.

Efficient transient delivery of FLP recombinase into various cell types

To further explore the potential of the improved RMT vectors, we replaced SB by the codon-optimized FLPo (15), produced particles as above, and transduced HT1080 indicator cells harboring two lentivirally transduced copies of a reporter gene in which FLP-mediated excision of EGFP induces expression of dTomato (Supplementary Figure S5A and B). The conversion of green to red fluorescence is a reliable indicator of FLP

Figure 1. Continued

Spleen Focus Forming Virus (SFFV). To improve RMT, the 5' MPSV promoter was replaced by the Rous Sarcoma Virus (RSV) U3 (pRSF91aPBS, vector 2). To further enhance SB expression levels, the 900 bp fragment of the Woodchuck Hepatitis Virus post-transcriptional-regulatory element (PRE) containing polyadenylation enhancer sequences was inserted (pRSF91aPBS+PRE, vector 3). (B) Bluescript plasmids (pSK) harboring the transposable elements (TE) were used in this study. SFFV driven expression cassettes encoding either for EGFP (pSK.IR.SF.EGFP.pA.IR) or the red fluorescent mCherry (pSK.IR.SF.mCherry.pA.IR) protein are flanked by the so-called inverted and directed repeats (IR and DR, respectively), the recognition sites of the SB transposase. The resulting transcripts are terminated by the introduction of the SV40 polyadenylation signal (pA). (C) Northern blot analysis of transfected 293 T cells. All three types of SB variants (cSB, SB100X and SB100Xo) were tested in each vector setting: pSF91aPBS (1), pRSF91aPBS (2) and pRSF91aPBS+PRE (3). RNA was harvested 36 h post-transfection and probed against the 3' SFFV U3 region. 18S RNA served as a loading control. The upper band of each lane corresponds to the unspliced RNA and the lower band reflects the spliced species. (D) Correlation of relative RNA and protein levels of SB100X and SB100Xo constructs. Levels of pSF91aPBS.SB100X (SB100X vector 1) were set to 100%. (E) Efficient RMT mediated SB transposition in HeLa cells. The HeLa cells were first transduced with 5 μ l SF91aPBS or RSF91aPBS or RSF91aPBS+PRE SB100Xo particles and then transfected 22 h later with a plasmid harboring the transposable element encoding for EGFP. FACS plots of cells analyzed 2 and 21 days post-transfection are depicted. Cells only transfected (Trf.) with the transposable element served as control. (F) Summary of three independent experiments with increasing levels of viral supernatants as used in (E). RSF91aPBS.SB100Xo.PRE supernatants generated without (w/o) Gag/Pol served as control for protein or plasmid carry-over from the packaging cell. The light gray shaded area indicates mean background plasmid integration levels of the transposable element.

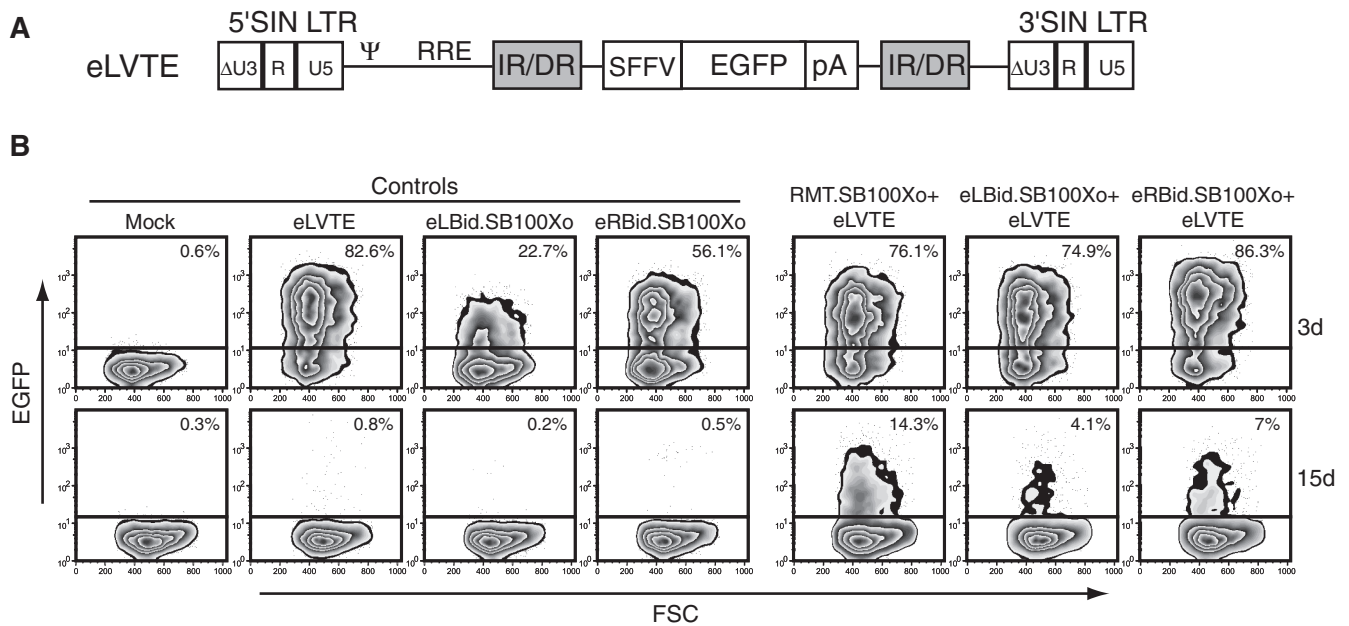


Figure 2. Cotransduction of RMT.SB100Xo and episomal lentiviral vector particles delivering the transposable element results in efficient transposition in HeLa cells. (A) Lentiviral self inactivating (SIN, Δ U3) vector backbone harboring the transposable element (TE) expression cassette as shown in Figure 1B. RRE, rev responsive element; Ψ , packaging signal. To obtain integration-defective episomal lentiviral TE particles (eLVTE), the vector was packaged with a Gag/Pol mutant harboring the D64V mutation within the core domain of the viral integrase. (B) HeLa cells were cotransduced with 10 μ l concentrated eLVTE (MOI 3.5) and 30 μ l concentrated RMT.SB100Xo (RSF91 + PRE), or unconcentrated episomal bidirectional lentiviral or retroviral SB100Xo (eLBid.SB100Xo, eRBid.SB100Xo; both MOI 0.3) particles. Cells were analyzed via flow cytometry 3 and 15 days post-transduction. Cells that were only transduced with eLVTE or eLBid.SB100Xo or eRBid.SB100Xo served as controls for background integration events.

activity in these cells (17). Very similar to the data obtained with SB, the modification of the promoter and the insertion of the PRE synergistically increased FLPo delivery, leading to a 50-fold increased potency of both, RMT and iRV (Figure 3A and B). Titration experiments revealed that a 25-fold higher volume of vector supernatant was needed for RMT in comparison to iRV. This is remarkable, as each retroviral particle contains only two copies of the plus-stranded mRNA genome. Furthermore, we tested FLPo delivery by episomal gammaretroviral and lentiviral bidirectional vectors (eRBid.FLPo, eLBid.FLPo) and found these to mediate efficient and reproducible recombination of SC-1 based cells carrying one FLP reporter allele (Figure 3C–E and Supplementary Figure S5B). Next, we investigated the potency of RMT to deliver FLPo by transducing SC-1 fibroblasts or murine IPS, both containing the FLP reporter. An integrating gammaretroviral vector encoding FLPo served as positive control. With a strictly dose-dependent performance, RMT reached a high efficiency: we obtained >95% recombined SC-1 fibroblasts (Supplementary Figure S5C) and ~40% recombined IPS cells (MOI ~40, Figure 3F). Thus, RMT efficiently delivers different types of DNA-modifying enzymes (SB transposase and FLP recombinase) into various cell types.

Dose-dependent cytotoxicity of SB transposase

In the course of all experiments, integrating gammaretroviral and lentiviral vectors (uni- or bidirectional)

expressing cSB, SB100X, SB100Xo or FLPo served as positive controls. However, in cultured cells stably transduced by these vectors, we observed pronounced cytotoxicity with either of the SB variants. Cytotoxicity was accompanied by low transposition rates (Supplementary Figure S6A and B) due to increased cell death occurring within a few days after transduction (Supplementary Figure S6C and D). Cytotoxicity only depended upon the delivery of the transposase, and occurred in the absence of a co-delivered transposable element. As SB is not known to recognize endogenous transposable elements of the human genome (27) continued transposition was an unlikely explanation for the observed toxicity.

To further examine the cytotoxic effects, we used the most potent integrating or RMT vector setting to transduce HeLa cells and monitored the corresponding SB protein expression levels 3 and 22 h as well as 12 days after transduction (Figure 4A). To ensure equal particle load, all cells were additionally analyzed for retroviral capsid protein (p30) and retroviral genomic mRNA levels at early (3 h) and late (p30: 22 h and 12 day; genomic mRNA: 22 h) time points (Figure 4A and B). Whereas SB expression was barely visible in all cell lysates harvested 3 h post-transduction, it was clearly detectable in cells, transduced by iRV or RMT particles, 22 h after transduction (Figure 4A). However, SB expression from iRV vectors decreased over time (12 day), correlating with decreased levels of proviral genomic DNA (Figure 4A and C). These

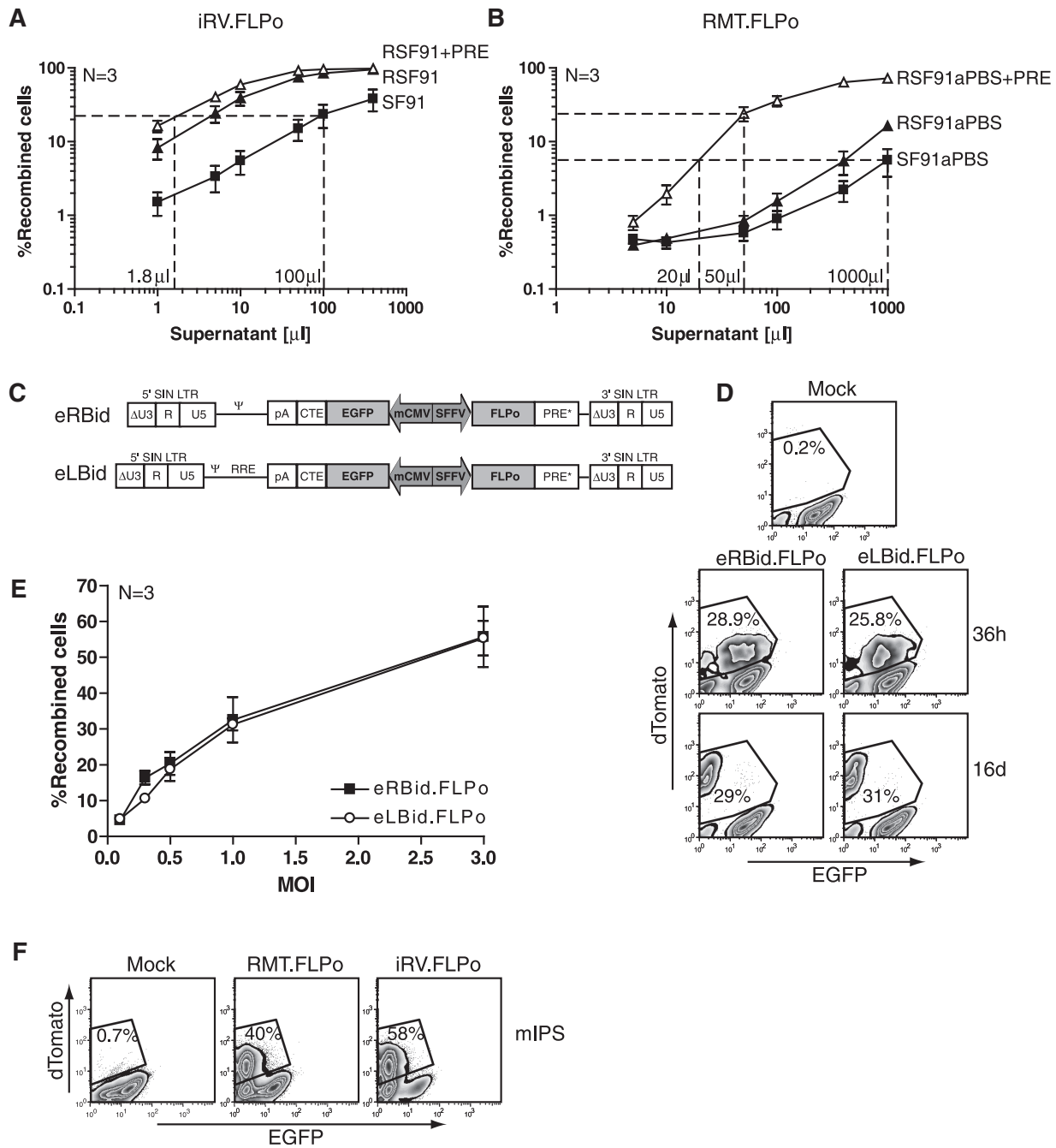


Figure 3. Optimization of the retroviral integrating and RMT vector backbones enhances FLPo-mediated recombination. (**A** and **B**) Human HT1080-derived FLP indicator cells harboring two lentivirally transduced copies of a FLP reporter gene [with conversion of EGFP to dTomato expression after FLP exposure, (17)] were transduced with integrating retroviral (iRV) or RMT particles encoding for codon-optimized FLPo expressed from different vector backbones (see also Figure 1A). The graphs display the percentage of recombined cells in relation to the amount of non-concentrated supernatant used. (**C**) Schematic overview of episomal bidirectional lentiviral and gammaretroviral SIN vectors coexpressing FLPo and EGFP (eLBid.FLPo, eRBid.FLPo). Both vectors consist of two independent transcription units: SFFV promoter driven FLPo is expressed in sense and terminated at the viral's polyadenylation signal (pA) located within R of the 3'LTR. EGFP is cloned in antisense orientation to the vector backbone and is expressed by a minimal CMV (mCMV) promoter that is *trans*-activated by SFFV. The EGFP antisense transcript is terminated by the SV40 polyadenylation signal (pA). To facilitate nuclear export the constitutive transport element (CTE) of Mason-Pfizer Monkey Virus was inserted. PRE*: 600 bp post-transcriptional element of the Woodchuck Hepatitis Virus, devoid of the X open reading frame (18). (**D** and **E**) Efficient FLPo transfer using eLBid.FLPo and eRBid.FLPo particles. Murine SC-1-based FLP indicator cells harboring one copy of the FLP reporter allele were transduced with increasing MOIs as depicted and analyzed via flow cytometry for recombination efficiencies (**E**). Representative FACS plots of transduced cells (MOI 1) 36h and 16days post-transduction (**D**). (**F**) Efficient transient FLPo transfer into murine induced pluripotent stem cells (mIPSC). RMT.FLPo and iRV.FLPo particles were titrated on murine FLP indicator cells (see also Supplementary Figure S5) and the percentage of recombined cells was used for titer determination. Murine IPS cells harboring the FLP indicator expression cassette were transduced with both particle types at an MOI of 40. Non-recombined EGFP expressing cells are shown on the *x*-axis and recombined dTomato expressing cells on the *y*-axis.

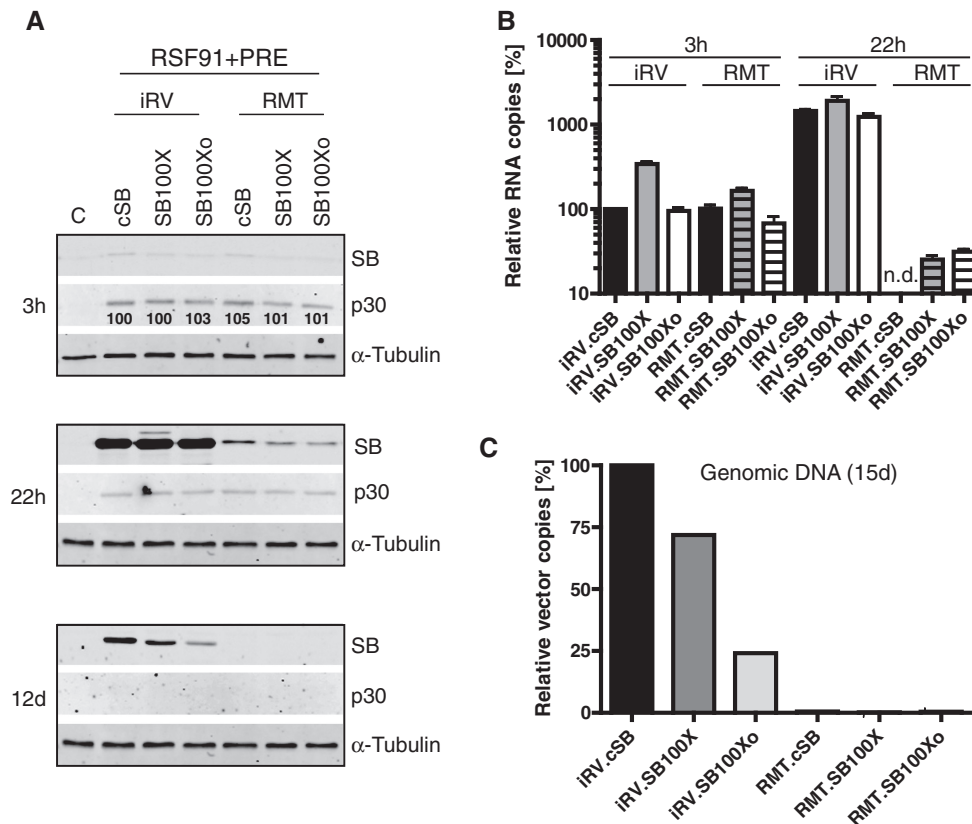


Figure 4. RMT-mediated SB expression is transient and non-toxic. (A) Western blot analysis of transduced HeLa cells. Choosing the most potent vector backbones (RSF91aPBS+PRE or RSF91+PRE), HeLa cells were transduced with RMT and integrating retroviral vector (iRV) particles encoding either for cSB, SB100X or SB100Xo. Cell lysates were prepared 3 h, 22 h and 12 days post-transduction and analyzed for SB transposase and retroviral capsid (p30) expression levels. α -Tubulin protein expression levels served as loading control. Relative p30 levels (%) in cells that were harvested 3 h post-transduction are indicated. They were determined and normalized to α -tubulin expression levels. RSF91.cSB.PRE was set to 100%. (B) Retroviral vector RNA levels early (3 h) and late (22 h) after cellular entry. Total RNA was harvested from cells shown in (A) and analyzed via real-time RT-PCR for relative vector mRNA levels 3 and 22 h post-transduction (value for iRV.cSB was set to one). The value for RMT of cSB was not determined (n.d.). (C) Detection of proviral vector DNA via quantitative PCR. To rule out plasmid contamination, genomic DNA was harvested 15 days post-transduction and analyzed by qPCR using primers directed against the PRE. The graph depicts relative vector levels. The value for iRV.cSB was set to 100%.

data suggested that persistent SB expression is cytotoxic and may lead to cell death.

Interestingly, when transducing cells with iRV, expression levels of SB and persistence of cells expressing SB were inversely correlated with the potency of the transposase variant (Figure 4A–C). In contrast, RMT led to a transient expression of SB, declining rapidly between 3 and 22 h (Figure 4B), and disappearing traceless in long-term cultivated cells at the level of both nucleic acid and protein (Figure 4A and C), without evidence for toxicity.

Cell death occurred in p53-low HeLa cells (28) and CF1 MEFs, where mortality increased up to 20% by Day 2 or 11 post-transduction, respectively and cell growth ceased in the surviving cells (Supplementary Figure S6C–F). Whereas cytotoxicity was observed with constitutive expression of SB100Xo, SB100X and cSB, continued expression of FLPo was only slightly more toxic than mock treatment (Supplementary Figure S6E). AnnexinV/propidium iodide (PI) costaining 2 days post-transduction indicated that SB-mediated cell loss was mainly caused by apoptosis (Figure 5A and Supplementary Figure S6E),

whereas the proportion of AnnexinV⁺ cells was minor in cells transduced with the same bidirectional retroviral expression constructs encoding FLPo or a truncated version of the CD34 receptor [tCD34, (29)] (Supplementary Figure S7A and B). Interestingly, even transient expression of SB100X or SB100Xo from episomal bidirectional vectors induced apoptosis, which was dependent on the dose of the transposase (Supplementary Figure S7C). This toxicity may have contributed to the reduced potency of eLV compared to RMT for delivery of SB, as indicated in the above experiments (Figure 2).

SB-mediated cytotoxicity is preceded by a G2/M cell cycle arrest

When transducing HeLa Fucci cells that allow the monitoring of cell cycle stages by expressing monomeric versions of the fluorescent proteins Kusabira Orange (mKO2) and Azami Green [mAG, Figure 5B; (16)] a pronounced pre-mitotic cell cycle arrest in the S/G2/M cell fraction became apparent 2–3 days post-transduction (upper left quadrants in Figure 5C). A new population

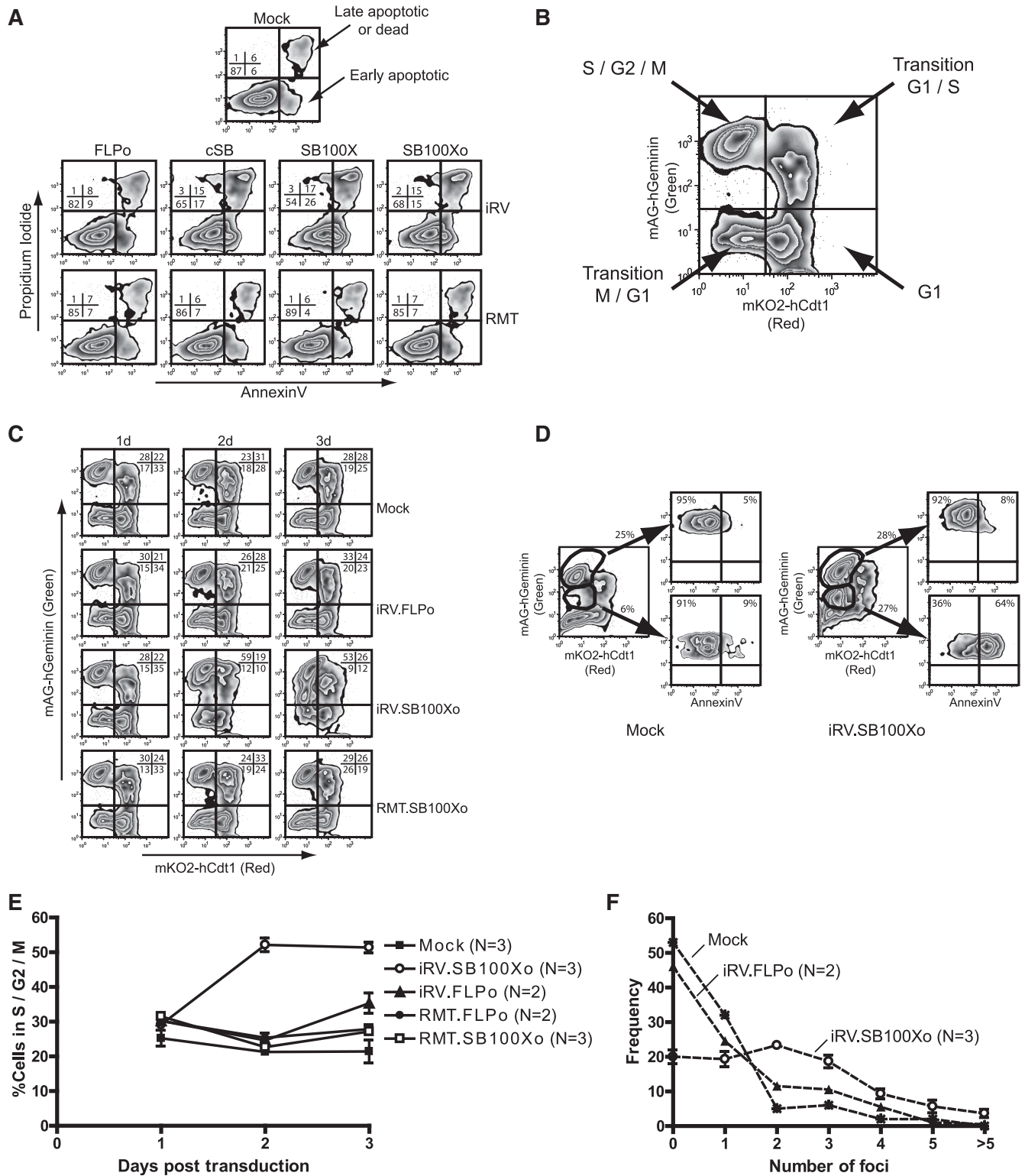


Figure 5. Constitutive expression of SB transposase is cytotoxic. **(A)** HeLa cells were transduced with iRV and RMT vectors (RSF91+PRE or RSF91aPBS+PRE) encoding either for codon-optimized FLPo, cSB, SB100X and codon-optimized SB100Xo. Two days post-transduction cells were stained for early apoptotic and late apoptotic/dead cells using propidium iodide and AnnexinV staining and analyzed via flow cytometry. **(B)** Typical FACS plot of HeLa Fucci cells (16). Due to the cell cycle-dependent inverse oscillation of both fusion proteins (orange mKO2-hCdt1 and green mAG-hGeminin), the nuclei of HeLa Fucci cells being within G1 are labelled in red, whereas nuclei in S/G2/M phases are represented by green fluorescence. The transition of G1/S results in mKO2-hCdt1 and mAG-hGeminin double positive nuclei and the transition of M/G1 is indicated by unstained nuclei. **(C)** Constitutive SB100Xo expression leads to a G2/M arrest. HeLa Fucci cells were transduced with integrating iRV.FLPo, iRV.SB100Xo or RMT particles encoding for SB100Xo (all RSF91+PRE). One to three days post-transduction cells were analyzed via flow cytometry. **(D)** The additional population observed in **(C)** represents apoptotic (AnnexinV⁺) cells. HeLa Fucci cells were transduced with integrating iRV.SB100Xo and analyzed on Day 3 after transduction. **(E)** Summary of 2–3 independent experiments showing the premitotic arrest in cells

(continued)

with weak expression of the endogenous cell cycle marker, Geminin-mAG, was observed in cells transduced with SB100Xo vectors three days post-transduction (located toward the bottom of the upper left quadrants in Figure 5C), and this population was AnnexinV⁺ (Figure 5D). Quantification of the flow cytometry plots showed that transduction with iRV expressing SB100Xo doubled the proportion of cells in S/G2/M compared to controls (iRV expressing FLPo or RMT of either SB100Xo or FLPo), already at Day 2 post-transduction (Figure 5E). When encoding FLPo, RMT avoided the induction of a relatively mild pre-mitotic arrest that was detectable on Day 3 when using integrating expression vectors (Figure 5E).

Since Geminin is one of the direct substrates of the cell cycle regulating ubiquitin-protein ligase anaphase-promoting-complex, which is mainly active in mitosis and the G1 phase of the cell cycle (16), the accumulation of single positive Geminin-mAG cells strongly suggests that prolonged and high-level expression of the transposase perturbs the progression from G2 into mitosis (Figure 5C). Our data thus reveal a dose-dependent G2/M cell cycle arrest and induction of apoptosis caused by the overexpressed transposase. In addition, these experiments demonstrate the utility of Fucci cells (16) to indicate both, alterations of cell cycle progression caused by an overexpressed DNA modifying enzyme and apoptotic cell populations.

SB-mediated cytotoxicity does not depend on its catalytic activity and can be prevented using caspase inhibitors

Pre-mitotic cell cycle arrest can be indicative of enhanced DNA repair. We thus performed γ H2AX stains, but found only moderately increased numbers of DNA repair foci after expressing SB from integrating vectors, whereas FLPo had no significant effect (Figure 5F). In order to better understand the apoptotic fate of cells transduced with SB, we additionally performed multiplex phosphoprotein expression analyses for a subset of signaling molecules that are key regulators of cellular stress responses. We thus found a highly significant induction of p53 and c-Jun (both total protein and phosphorylated forms), a trend to reduced total ERK1/2 protein levels, although phospho-ERK1/2 variants were increased at later time points (Figure 6D–F), and, always compared to the EGFP control, no major effect of SB100X on Akt, a marker of endoplasmic reticulum (ER) stress (30) (Supplementary Figure S8).

To explore whether cytotoxic effects of SB overexpression depended on its catalytic domain, we introduced and validated triple mutations of the DDE motif that is essential for the DNA-cleavage activity of the transposase (Figure 6A). As cell cycle arrest and apoptosis were only

slightly reduced compared to the enzymatically active SB100X, our data suggest that DNA cleavage is not the primary mechanism of cell cycle arrest and apoptosis (Figure 6B and C).

These results prompted us to analyze whether transposase-dependent cytotoxicity also occurs upon conventional transfection to deliver cSB, SB100X and SB100Xo, using the improved plasmids designed for generation of RMT particles (pRSF91aPBS+PRE, Figure 1A) or a standard expression vector [pCMV.SB100X, (2)]. Again, we observed an increase of apoptosis and cell death, which was reproducibly higher than the background toxicity of the transfection method (Supplementary Figure S9). Importantly, when using pRSF91aPBS.SB100X.PRE at the lowest plasmid dose required for efficient transposition (10 ng per well), cytotoxicity of SB100X was not exceeding the background toxicity of the transfection procedure. Finally, we were able to dissect SB's induction of cell cycle arrest and apoptosis by irreversibly inhibiting the caspase pathway using Q-VD-OPH (31), further indicating that apoptosis occurs as a consequence of the G2/M arrest (Figure 6G). Thus, in sum, transient and dose-controlled delivery of SB by RMT avoided cytotoxic effects (Figure 5 and Supplementary Figure S6), while mediating efficient integration of transposable elements delivered via either physicochemical transfection or episomal lentiviral vectors (Figures 1 and 2; Supplementary Figure S2 and S4).

DISCUSSION

The present study introduces an improved retroviral particle-mediated platform for efficient mRNA delivery of DNA-modifying enzymes such as the SB transposase or the FLP recombinase. Using a previous, less-efficient generation of RMT vectors, delivery of the Cre recombinase has been demonstrated (11). The efficiency of RMT correlates with the amount of retroviral mRNA genomes in viral particles (7). In the present study, we increased the potency of RMT by vector modifications that enhance the generation of vector mRNA in producer cells. We codon-optimized the SB100X cDNA and introduced the longest version of the Woodchuck Hepatitis Virus PRE (20,23), which among all PREs tested by us to date has the greatest effect on post-transcriptional mRNA processing, including transcriptional termination, polyadenylation and translation (21,22). The rationale for the long PRE and the codon-optimization of SB100X was not only to maximize RNA expression in packaging cells but also to enhance the efficiency of translation in target cells. Since expression levels are not a major limitation for DNA transfection-based delivery of

Figure 5. Continued

constitutively expressing SB100Xo. As additional control RMT.FLPo particles were included. (F) HeLa cells constitutively expressing SB100Xo show an increase in double strand breaks compared to Mock or FLPo expressing cells. Cells were analyzed 1 day post-transduction using the γ H2AX immunofluorescence assay. For iRV.SB100Xo (RSF91+PRE) three independent experiments were performed counting the foci of 100 nuclei each, for iRV.FLPo (RSF91+PRE) 2 × 100 nuclei and for Mock 1 × 100 nuclei were analyzed.

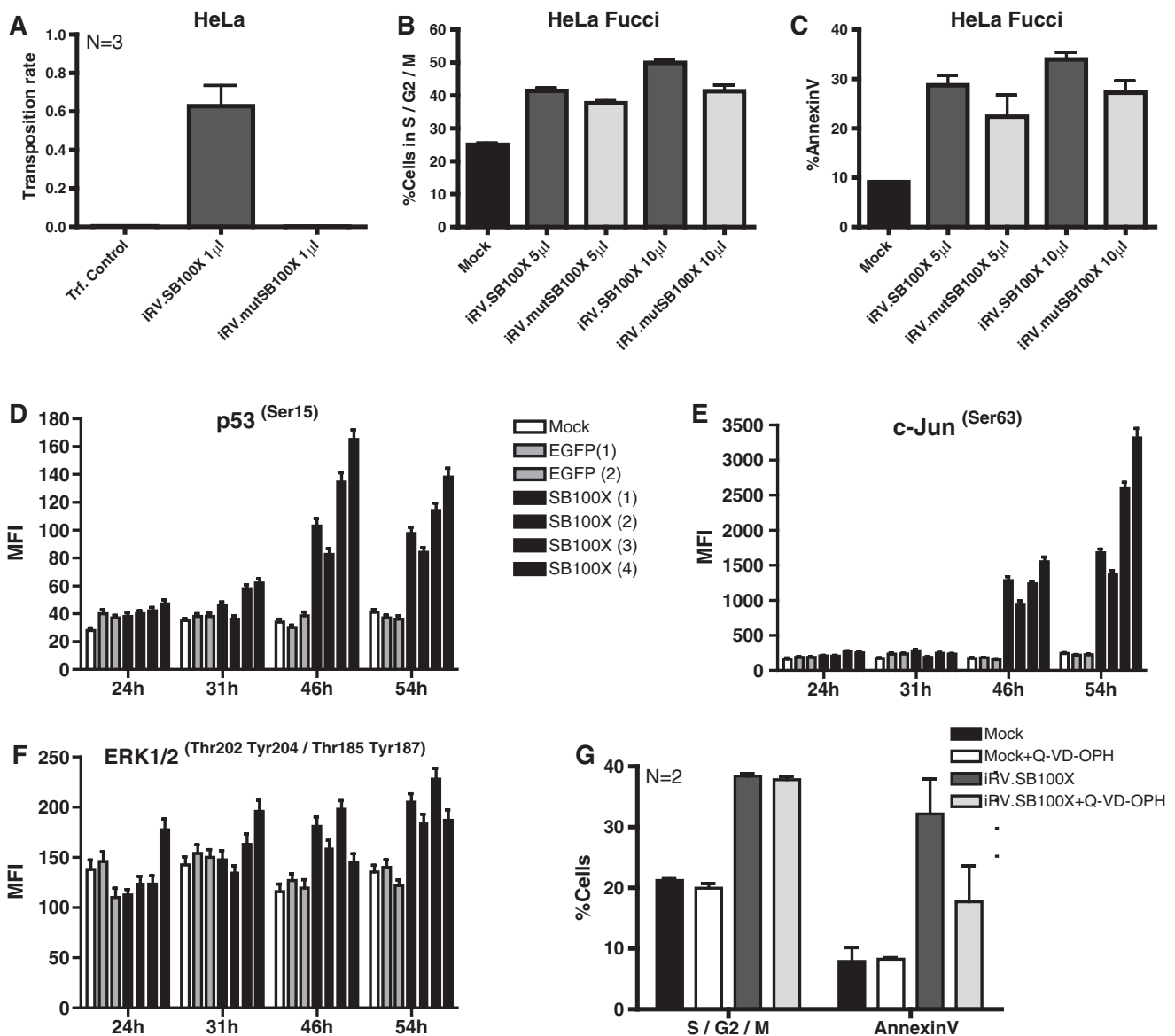


Figure 6. Analysis of cellular effects of SB100X overexpression. (A) Inactivation of the SB's catalytic domain by mutating the DDE motif completely inhibits transposition. To avoid excessive cytotoxicity HeLa cells were transduced with just 1 μ l (instead of 5 μ l) concentrated wild-type iRV.SB100X or mutant iRV.mutSB100X. The following day the transposable element plasmid pSK.IR.SF.EGFP.pA.IR was cotransfected. Cells were FACS analyzed for EGFP expression 2 and 23 days post-transfection and the resultant transposition rates were determined. Cells that were transfected in the absence of SB100X served as control for residual integration events of the transposable element plasmid (Trf. Control). (B and C) DDE mutated SB100X just slightly reduces cytotoxicity. HeLa Fucci cells were transduced with 5 or 10 μ l concentrated iRV.SB100X or the corresponding DDE motif mutant. Two days post-transduction cells were stained with AnnexinV and analyzed for the percentage of cells being either within S/G2/M (A) or AnnexinV positive (B). Except for untreated cells (Mock, $N = 2$) three independent experiments are shown, respectively. (D–F) Overexpression of SB transposase leads to enhanced phosphorylation of p53, c-Jun and ERK1/2 in HeLa cells. HeLa cells were transduced with four different preparations integrating iRV.SB100X (RSF91+PRE, dark gray bars) or two preparations of corresponding integrating iRV.EGFP supernatants (light gray bars). Untreated HeLa cells served as mock control (white bar). Cells were lysed within culture plates at the indicated time points and subjected to phosphoplex analysis. Four different signaling molecules (p53, c-Jun, ERK1/2 and Akt) have been analyzed for total and phosphoprotein levels, however only the phosphorylation status of p53 (D), c-Jun (E) and ERK1/2 (F) are shown. The corresponding total protein levels as well as total and phosphoprotein levels of Akt are depicted in Supplementary Figure S8. Error bars reflect the standard deviation of the MFI of > 50 events. (G) The G2/M arrest induced by SB overexpression is independent from apoptosis. HeLa Fucci cells were transduced with 5 μ l concentrated iRV.SB100X in the presence or absence of the caspase inhibitor Q-VD-OPH (5 μ M). Two days post-transduction the percentage of cells in S/G2/M or those being AnnexinV positive were determined. The error bars show the standard deviation of the mean of two independent experiments.

SB, these modifications are of special interest for mRNA transduction methods.

At first glance, it may appear ironic to deliver a transposase, designed as a nonviral alternative of an

integrating vector, in the form of mRNA released from RT-deficient retroviral particles. However, as demonstrated in this study, the RMT approach introduced a potent, well-tolerated and non-cytotoxic

platform for dose-controlled and short-lasting expression of the SB transposase. Importantly, we found that prolonged, high-level expression of the transposase from episomal or integrating vectors not only resulted in reduced cell growth, but also triggered apoptosis in a dose-dependent manner. The considerable cytotoxicity of physicochemical transfection methods, previously used by most investigators to deliver transposases as plasmids or in the form of purified mRNA, may have masked toxic effects of overexpressed transposase.

Our detailed studies, using the recently introduced HeLa Fucci cells which allow color-coded cell cycle analyses (16), surprisingly revealed that apoptosis induced by SB overexpression is preceded by a substantial G2/M arrest. Irreversible inhibition of the caspase pathways by Q-VD-OPH further supported that apoptosis is secondary to the pre-mitotic cell cycle arrest. In addition, we observed substantial induction of p53 and c-Jun as well as increased numbers of γ H2AX foci. Phosphorylation of p53 at serine 15 and c-Jun at serine 63 are signaling events that indicate DNA damage and/or other forms of cellular stress (32,33). Our results might indicate that the observed cytotoxicity is a consequence of double-strand breaks induced by off-target cleavage events mediated by SB. However, γ H2AX foci in cells overexpressing SB were only moderate when compared to untreated cells and despite the generally accepted view of γ H2AX being a marker of double strand break repair, DNA damage-independent functions of γ H2AX have been suggested (34). Furthermore, inactivation of SB's catalytic domain (triple mutant of DDE motif) only slightly reduced cytotoxicity, further arguing against un-directed DNA cleavage by SB in the absence of the transposable element. Notably, the G2/M arrest may not always be triggered by DNA damage and can be also induced by other pathways inducing p53 (35–37). The phosphoprotein signature of Akt gave no evidence for ER stress-induced apoptosis mediated by potentially unfolded or misfolded proteins. However, SB overproduction may also induce other forms of misfolded protein responses in the cytosol or nucleus (38) or interfere with cell cycle progression by other mechanisms not involving its catalytic domain. Therefore, the exact mechanism of cell cycle arrest and apoptosis induced by SB overexpression remains to be defined. It is reassuring to note that the ectopic expression of the SB transposase was not found to be sufficient to cause developmental defects or cancer in experimental animals (39). Furthermore, our data indicate that cell stress induced by SB overexpression is likely to be self-limiting due to the induction of cell death with elimination of affected cells from a polyclonal cell pool.

By reducing the level and duration of transposase expression, RMT and dose-adapted transfection could prevent toxicity and should also reduce the rate of secondary transposition events, which may be caused by excision and re-integration of the transposon (40). Importantly, we demonstrate that SB-dependent cytotoxicity can be avoided without compromising efficacy, a finding that is likely to be similarly relevant for other methods of transposase delivery and other types of transposons. The

RMT platform should also be applicable to other transposases [such as *PiggyBac* (41) or *Frog Prince* (42)]. Furthermore, RMT was also found to efficiently transduce the FLP recombinase, again avoiding residual toxic effects that could be detected in our sensitive assay systems.

Other approaches for transient and dose-controlled delivery of DNA-modifying enzymes may rely on mRNA transfection, membrane-permeable proteins (43) or virus-like particles (17). The latter shares an important conceptual advantage with RMT: as shown in previous studies (11,17), retrovirus particle-mediated delivery of mRNA or protein can be confined to specific cell types by the choice of the viral envelope protein. Taking advantage of novel pseudotyping strategies (44), an increasing variety of cell types may be targeted. As exemplified with SB and FLPo, the here introduced optimized RMT vectors represent an efficient platform for transient cell manipulation, and are of special interest for approaches that benefit from a transient expression of proteins for genome modification.

SUPPLEMENTARY DATA

Supplementary Data are available at NAR Online.

ACKNOWLEDGEMENTS

The authors thank Ivonne Fernandez, Valerie Mordhost, Maimona Id, Girmay Asgedom, Diana Knetsch and Ludmila Umansky for technical assistance and Stefan Maßen for analysis and statistics of the Bio-Plex data.

FUNDING

Grants of the Deutsche Forschungsgemeinschaft [SFB738 project C4 and excellence cluster REBIRTH], the Helmholtz Alliance Immunotherapy of Cancer DFG TRR77 [project A3], the German Ministry for Research and Education [BMBF] and the European Union [FP7 integrated project PERSIST]. Funding for open access charges: SFB738.

Conflict of interest statement. None declared.

REFERENCES

- Ivics,Z., Hackett,P.B., Plasterk,R.H. and Izsvak,Z. (1997) Molecular reconstruction of Sleeping Beauty, a Tc1-like transposon from fish, and its transposition in human cells. *Cell*, **91**, 501–510.
- Mates,L., Chuah,M.K., Belay,E., Jerchow,B., Manoj,N., Acosta-Sanchez,A., Grzela,D.P., Schmitt,A., Becker,K., Matrai,J. *et al.* (2009) Molecular evolution of a novel hyperactive Sleeping Beauty transposase enables robust stable gene transfer in vertebrates. *Nat. Genet.*, **41**, 753–761.
- Hackett,P.B., Largaespada,D.A. and Cooper,L.J. (2010) A transposon and transposase system for human application. *Mol. Ther.*, **18**, 674–683.
- Dull,T., Zufferey,R., Kelly,M., Mandel,R.J., Nguyen,M., Trono,D. and Naldini,L. (1998) A third-generation lentivirus vector with a conditional packaging system. *J. Virol.*, **72**, 8463–8471.

5. Izsvak,Z., Ivics,Z. and Plasterk,R.H. (2000) Sleeping Beauty, a wide host-range transposon vector for genetic transformation in vertebrates. *J. Mol. Biol.*, **302**, 93–102.
6. Izsvak,Z. and Ivics,Z. (2004) Sleeping beauty transposition: biology and applications for molecular therapy. *Mol. Ther.*, **9**, 147–156.
7. Galla,M., Schambach,A., Towers,G.J. and Baum,C. (2008) Cellular restriction of retrovirus particle-mediated mRNA transfer. *J. Virol.*, **82**, 3069–3077.
8. Stephen,S.L., Montini,E., Sivanandam,V.G., Al-Dhalimy,M., Kestler,H.A., Finegold,M., Grompe,M. and Kochanek,S. (2010) Chromosomal integration of adenoviral vector DNA in vivo. *J. Virol.*, **84**, 9987–9994.
9. Nightingale,S.J., Hollis,R.P., Pepper,K.A., Petersen,D., Yu,X.J., Yang,C., Bahner,I. and Kohn,D.B. (2006) Transient gene expression by nonintegrating lentiviral vectors. *Mol Ther.*, **13**, 1121–1132.
10. Wilber,A., Wangenstein,K.J., Chen,Y., Zhuo,L., Frandsen,J.L., Bell,J.B., Chen,Z.J., Ekker,S.C., McIvor,R.S. and Wang,X. (2007) Messenger RNA as a source of transposase for sleeping beauty transposon-mediated correction of hereditary tyrosinemia type I. *Mol. Ther.*, **15**, 1280–1287.
11. Galla,M., Will,E., Kraunus,J., Chen,L. and Baum,C. (2004) Retroviral pseudotransduction for targeted cell manipulation. *Mol. Cell*, **16**, 309–315.
12. Lund,A.H., Duch,M., Lovmand,J., Jorgensen,P. and Pedersen,F.S. (1997) Complementation of a primer binding site-impaired murine leukemia virus-derived retroviral vector by a genetically engineered tRNA-like primer. *J. Virol.*, **71**, 1191–1195.
13. Hildinger,M., Abel,K.L., Ostertag,W. and Baum,C. (1999) Design of 5' untranslated sequences in retroviral vectors developed for medical use. *J. Virol.*, **73**, 4083–4089.
14. Philpott,N.J. and Thrasher,A.J. (2007) Use of nonintegrating lentiviral vectors for gene therapy. *Hum. Gene Ther.*, **18**, 483–489.
15. Raymond,C.S. and Soriano,P. (2007) High-efficiency FLP and PhiC31 site-specific recombination in mammalian cells. *PLoS One*, **2**, e162.
16. Sakaue-Sawano,A., Kurokawa,H., Morimura,T., Hanyu,A., Hama,H., Osawa,H., Kashiwagi,S., Fukami,K., Miyata,T., Miyoshi,H. *et al.* (2008) Visualizing spatiotemporal dynamics of multicellular cell-cycle progression. *Cell*, **132**, 487–498.
17. Voelkel,C., Galla,M., Maetzig,T., Warlich,E., Kuehle,J., Zychlinski,D., Bode,J., Cantz,T., Schambach,A. and Baum,C. (2010) Protein transduction from retroviral Gag precursors. *Proc. Natl Acad. Sci. USA*, **107**, 7805–7810.
18. Maetzig,T., Galla,M., Brugman,M.H., Loew,R., Baum,C. and Schambach,A. (2010) Mechanisms controlling titer and expression of bidirectional lentiviral and gammaretroviral vectors. *Gene Ther.*, **17**, 400–411.
19. Izsvak,Z., Stuwe,E.E., Fiedler,D., Katzer,A., Jeggo,P.A. and Ivics,Z. (2004) Healing the wounds inflicted by sleeping beauty transposition by double-strand break repair in mammalian somatic cells. *Mol. Cell*, **13**, 279–290.
20. Schambach,A., Mueller,D., Galla,M., Versteegen,M.M., Wagemaker,G., Loew,R., Baum,C. and Bohne,J. (2006) Overcoming promoter competition in packaging cells improves production of self-inactivating retroviral vectors. *Gene Ther.*, **13**, 1524–1533.
21. Schambach,A., Galla,M., Maetzig,T., Loew,R. and Baum,C. (2007) Improving transcriptional termination of self-inactivating gamma-retroviral and lentiviral vectors. *Mol. Ther.*, **15**, 1167–1173.
22. Higashimoto,T., Urbinati,F., Perumbeti,A., Jiang,G., Zarzuela,A., Chang,L.J., Kohn,D.B. and Malik,P. (2007) The woodchuck hepatitis virus post-transcriptional regulatory element reduces readthrough transcription from retroviral vectors. *Gene Ther.*, **14**, 1298–1304.
23. Hope,T. (2002) Improving the post-transcriptional aspects of lentiviral vectors. *Curr. Top Microbiol. Immunol.*, **261**, 179–189.
24. Kozak,M. (1987) An analysis of 5'-noncoding sequences from 699 vertebrate messenger RNAs. *Nucleic Acids Res.*, **15**, 8125–8148.
25. Staunstrup,N.H., Moldt,B., Mates,L., Villesen,P., Jakobsen,M., Ivics,Z., Izsvak,Z. and Mikkelsen,J.G. (2009) Hybrid lentivirus-transposon vectors with a random integration profile in human cells. *Mol. Ther.*, **17**, 1205–1214.
26. Vink,C.A., Gaspar,H.B., Gabriel,R., Schmidt,M., McIvor,R.S., Thrasher,A.J. and Qasim,W. (2009) Sleeping beauty transposition from nonintegrating lentivirus. *Mol. Ther.*, **17**, 1197–1204.
27. Izsvak,Z., Khare,D., Behlke,J., Heinemann,U., Plasterk,R.H. and Ivics,Z. (2002) Involvement of a bifunctional, paired-like DNA-binding domain and a transpositional enhancer in Sleeping Beauty transposition. *J. Biol. Chem.*, **277**, 34581–34588.
28. Scheffner,M., Munger,K., Byrne,J.C. and Howley,P.M. (1991) The state of the p53 and retinoblastoma genes in human cervical carcinoma cell lines. *Proc. Natl Acad. Sci. USA*, **88**, 5523–5527.
29. Fehse,B., Richters,A., Putimtseva_Scharf,K., Klump,H., Li,Z., Ostertag,W., Zander,A.R. and Baum,C. (2000) CD34 splice variant: an attractive marker for selection of gene-modified cells. *Mol. Ther.*, **1**, 448–456.
30. Hosoi,T., Hyoda,K., Okuma,Y., Nomura,Y. and Ozawa,K. (2007) Akt up- and down-regulation in response to endoplasmic reticulum stress. *Brain Res.*, **1152**, 27–31.
31. Caserta,T.M., Smith,A.N., Gultice,A.D., Reedy,M.A. and Brown,T.L. (2003) Q-VD-OPh, a broad spectrum caspase inhibitor with potent antiapoptotic properties. *Apoptosis*, **8**, 345–352.
32. Leppa,S. and Bohmann,D. (1999) Diverse functions of JNK signaling and c-Jun in stress response and apoptosis. *Oncogene*, **18**, 6158–6162.
33. Meek,D.W. (2009) Tumour suppression by p53: a role for the DNA damage response? *Nature Rev. Cancer*, **9**, 714–723.
34. Ismail,I.H. and Hendzel,M.J. (2008) The gamma-H2AX: is it just a surrogate marker of double-strand breaks or much more?. *Environ. Mol. Mutagenesis*, **49**, 73–82.
35. Slebos,R.J. and Taylor,J.A. (2001) A novel host cell reactivation assay to assess homologous recombination capacity in human cancer cell lines. *Biochem. Biophys. Res. Comm.*, **281**, 212–219.
36. Teodoro,J.G., Heilman,D.W., Parker,A.E. and Green,M.R. (2004) The viral protein Apoptin associates with the anaphase-promoting complex to induce G2/M arrest and apoptosis in the absence of p53. *Genes Dev.*, **18**, 1952–1957.
37. Brand,K., Klocke,R., Possling,A., Paul,D. and Strauss,M. (1999) Induction of apoptosis and G2/M arrest by infection with replication-deficient adenovirus at high multiplicity of infection. *Gene Ther.*, **6**, 1054–1063.
38. Kubota,H. (2009) Quality control against misfolded proteins in the cytosol: a network for cell survival. *J. Biochem.*, **146**, 609–616.
39. Copeland,N.G. and Jenkins,N.A. (2010) Harnessing transposons for cancer gene discovery. *Nat. Rev. Cancer*, **10**, 696–706.
40. Liang,Q., Kong,J., Stalker,J. and Bradley,A. (2009) Chromosomal mobilization and reintegration of Sleeping Beauty and PiggyBac transposons. *Genesis*, **47**, 404–408.
41. Wilson,M.H., Coates,C.J. and George,A.L. Jr (2007) PiggyBac transposon-mediated gene transfer in human cells. *Mol. Ther.*, **15**, 139–145.
42. Miskey,C., Izsvak,Z., Plasterk,R.H. and Ivics,Z. (2003) The Frog Prince: a reconstructed transposon from *Rana pipiens* with high transpositional activity in vertebrate cells. *Nucleic Acids Res.*, **31**, 6873–6881.
43. Edenhofer,F. (2008) Protein transduction revisited: novel insights into the mechanism underlying intracellular delivery of proteins. *Curr. Pharm. Des.*, **14**, 3628–3636.
44. Buchholz,C.J., Muhlebach,M.D. and Cichutek,K. (2009) Lentiviral vectors with measles virus glycoproteins - dream team for gene transfer? *Trends Biotechnol.*, **27**, 259–265.